

Aliphatic C–H Bond Oxygenation by the Co^{II}OOX Species with the Hindered Hydrotris(pyrazolyl)borate Ligand (X = Co(II), Alkyl, H)

Shiro Hikichi,* Hidehito Komatsuzaki, Munetaka Akita, and Yoshihiko Moro-oka*

Contribution from the Research Laboratory of Resources Utilization, Tokyo Institute of Technology, 4259 Nagatsuta, Midori-ku, Yokohama 226-8503, Japan

Received June 23, 1997

Abstract: Aliphatic C–H bond oxygenation is achieved by Co(II)–peroxo species. The dinuclear Co(II)– μ -peroxo complex, {Co[HB(3,5-Prⁱpz)₃]₂(μ -O₂)} (2), is yielded by reaction of the bis(μ -hydroxo)–Co(II) complex, {Co(OH)[HB(3,5-Prⁱpz)₃]₂} (1), with an equimolar amount of H₂O₂. Spontaneous decomposition of the μ -peroxo complex 2 yields a mono-oxygenated μ -alkoxo- μ -hydroxo complex, Co₂(μ -OH)[HB(μ -3-OCMe₂-5-Prⁱpz)(3,5-Prⁱpz)₂][HB(3,5-Prⁱpz)₃] (4), in which one of the six 3-isopropyl methine carbon atoms is oxygenated and the resulting alkoxo ligand bridges the two Co(II) centers. In contrast, decomposition of 2 in the presence of an excess amount of H₂O₂ results in further oxygenation to give a mixture of the dinuclear Co(II)–bis(μ -alkoxo) complex, {Co[HB(μ -3-OCMe₂-5-Prⁱpz)(3,5-Prⁱpz)₂]₂} (5), and the mononuclear Co(II)–hydroxo alcohol complex, Co(OH)[HB(3-Me₂COH-5-Prⁱpz)(3-Me₂COH-5-Prⁱpz)₂] (6). In the bis(μ -alkoxo) complex 5, one of the three 3-isopropyl groups in each ligand is functionalized to give the alkoxide group, which bridges the two metal centers. In the mononuclear hydroxo alcohol complex 6, all of the three 3-isopropyl groups are oxygenated. The Co(II) center is coordinated by the resulting alcohol ligand as well as an hydroxide. Reaction of 1 with 2 equiv of ROOH (R = Bu^t and PhMe₂C) at low temperature yields the blue thermally unstable alkylperoxo compound 3. The HB(3-Bu^t-5-Prⁱpz)₃ derivative, Co(OOCMe₂-Ph)[HB(3-Bu^t-5-Prⁱpz)₃] (9), characterized successfully by X-ray crystallography contains the tetrahedral Co center. The monomeric alkylperoxo complexes 3 also decomposes to give the bis(μ -alkoxo) complex 5, but neither mono-oxygenated 4 nor fully oxygenated 6 is obtained. These observations suggest that the present aliphatic C–H bond oxygenations may proceed via homolysis of the O–O bond of the Co(II)–peroxo species.

Introduction

Aliphatic C–H bond functionalization associated with O–O bond activation on transition metal centers is the most attractive subject in the field of not only synthetic chemistry but also biochemistry.¹ In biological systems, heme and non-heme iron enzymes such as cytochrome P-450² and methane monooxygenase (MMO)^{3,4} catalyze hydroxylation of alkanes, giving

(1) (a) Arndtsen, B. A.; Bergman, R. G.; Mobley, T. A.; Peterson, T. H. *Acc. Chem. Res.* **1995**, 28, 154. (b) Sheldon, R. A.; Kochi, J. K., Eds. *Metal-Catalyzed Oxidations of Organic Compounds*; Academic Press: New York, 1981. (c) Gubelmann, M. H.; Williams, A. F. *Struct. Bonding* **1983**, 55, 1. (d) Special thematic issue on “Metal-Dioxygen Complexes”: *Chem. Rev.* **1994**, 94, 567–856. (e) Special thematic issue on “Bioinorganic Enzymology”: *Chem. Rev.* **1996**, 96, 2237–3042.

(2) (a) Sato, R.; Omura, T., Eds. *Cytochrome P-450*; Kodansha Ltd.: Tokyo, 1978. (b) White, R. E.; Coon, M. J. *Annu. Rev. Biochem.* **1980**, 49, 315. (c) Ortiz de Montellano, P. R., Ed. *Cytochrome P-450: Structure, Mechanism and Biochemistry*; Plenum Press: New York, 1986. (d) Watanabe, Y.; Groves, J. T. In *The Enzymes*; Sigman, Boyer, Eds.; Academic Press: Orlando, FL, 1992; pp 405–452. (e) Sono, M.; Roach, M. P.; Coulter, E. D.; Dawson, J. H. *Chem. Rev.* **1996**, 96, 2841.

(3) (a) Liu, K. E.; Lippard, S. J. *Adv. Inorg. Chem.* **1995**, 42, 263. (b) Rosenzweig, A. C.; Lippard, S. J. *Acc. Chem. Res.* **1994**, 27, 229. (c) Feig, A. L.; Lippard, S. J. *Chem. Rev.* **1994**, 94, 759. (d) Lipscomb, J. D. *Annu. Rev. Microbiol.* **1994**, 48, 371. (e) Andersson, K. K.; Gräslund, A. *Adv. Inorg. Chem.* **1995**, 43, 359. (f) Wallar, B. J.; Lipscomb, J. D. *Chem. Rev.* **1996**, 96, 2625.

(4) (a) Liu, K. E.; Valentine, A. M.; Qiu, D.; Edmondson, D. E.; Appelman, E. H.; Spiro, T. G.; Lippard, S. J. *J. Am. Chem. Soc.* **1995**, 117, 4997. (b) Shu, L.; Nesheim, J. C.; Kauffmann, K.; Münck, E.; Lipscomb, J. D.; Que, L., Jr. *Science* **1997**, 275, 515.

corresponding alcohols. It is suggested that metal–peroxo (O₂²⁻ and OOH⁻) species are formed prior to O–O and C–H bond activation in these processes.⁴

To elucidate the mechanism of O₂ activation by metal ions, the structure and reactivity of transition metal complexes with activated oxygen species (O₂⁻, O₂²⁻, OOH⁻, OOR⁻, and OOC(O)R⁻: peroxo species⁵) have attracted increasing attention. In our laboratory, Cu–, Fe–, and Mn–peroxo⁵ complexes with the hydrotris(3,5-diisopropylpyrazol-1-yl)borate [HB(3,5-Prⁱpz)₃] ligand have been investigated as biomimetic models.^{6–9} One of our remarkable results is the isolation and structural characterization of the first example of the Cu(II)₂– μ - η^2 : η^2 -peroxo complex which fully reproduces the spectroscopic characteristics of oxyhemocyanin and oxytyrosinase. It is notable that the unusual low ν (O–O) values for the model complex and the proteins are associated with the μ - η^2 : η^2 coordination mode of peroxo ion.^{7a–e,10} More recently, Tolman et al. have

(5) In this paper, “peroxide” refers to superoxide (O₂⁻), hydroperoxide (OOH⁻), alkyl peroxide (OOR⁻), and acyl peroxide (OOC(O)R⁻) species.

(6) Kitajima, N.; Tolman, W. B. *Prog. Inorg. Chem.* **1995**, 43, 419.

(7) Cu complexes: (a) Kitajima, N.; Moro-oka, Y. *Chem. Rev.* **1994**, 94, 737. (b) Kitajima, N.; Moro-oka, Y. *J. Chem. Soc., Dalton Trans.* **1993**, 2665. (c) Kitajima, N. *Adv. Inorg. Chem.* **1992**, 39, 1. (d) Kitajima, N.; Fujisawa, K.; Moro-oka, Y. *J. Am. Chem. Soc.* **1989**, 111, 8975. (e) Kitajima, N.; Fujisawa, K.; Fujimoto, C.; Moro-oka, Y.; Hashimoto, S.; Kitagawa, T.; Toriumi, K.; Tatsumi, K.; Nakamura, A. *J. Am. Chem. Soc.* **1992**, 114, 1277. (f) Kitajima, N.; Katayama, T.; Fujisawa, K.; Iwata, Y.; Moro-oka, Y. *J. Am. Chem. Soc.* **1993**, 115, 7872. (g) Kitajima, N.; Fujisawa, K.; Moro-oka, Y. *Inorg. Chem.* **1990**, 29, 357.

reported that the equilibrium between the $\text{Cu(II)}_2-\mu-\eta^2:\eta^2$ -peroxo and $\text{Cu(III)}-\text{bis}(\mu\text{-oxo})$ cores has been observed in the Pr^i_3TACN -copper complex containing a tripodal N_3M skeleton similar to that in the hydrotris(pyrazolyl)borate complexes (Pr^i_3TACN denotes 1,4,7-triisopropyl-1,4,7-triazacyclononane).¹¹ These observations suggest that the electronic and coordination environment of metal centers tuned by the supporting ligand are key factors for the O_2 activation mediated by metal complexes and motivate us to investigate the metal-dioxygen complexes systematically by using a series of the hydrotris(pyrazolyl)borate ligands. Recently we have extended our synthetic targets to dioxygen complexes of various transition metals. Comparison of the chemical and structural properties of various metal complexes may provide us insights into the reaction mechanisms, the roles of the metal ions in physiological oxygen metabolism and various chemical oxidation processes, directions for catalyst design, and so on.

Cobalt is the most studied element in the synthetic metal-dioxygen complexes, although no Co-dependent O_2 carrier and oxygenase is known so far. In cobalt-dioxygen complex chemistry, it is known that the common oxidation state of the metal center is Co(III) . In fact, many $\text{Co(III)}-\text{peroxo}^5$ complexes have been characterized,^{1c,12} but only a limited number of $\text{Co(II)}-\text{dioxygen}$ complexes such as mono- and dinuclear superoxo complexes and μ -peroxo complexes have been characterized.¹³ The first structurally characterized $\text{Co(II)}-\text{dioxygen}$ species is the monomeric superoxo complex bearing the highly sterically hindered hydrotris(pyrazolyl)borate ligand, $\text{Co(O}_2\text{)}-\text{[HB(3-Bu}^t\text{-5-Mepz)}_3]$, reported by Theopold et al.^{13a} They have

prepared another monomeric $\text{Co(II)}-\text{superoxo}$ complex, $\text{Co(O}_2\text{)}[\text{HB(3-Pr}^i\text{-5-Mepz)}_3]$, which shows unique behavior in solution; it gives the dimeric bis(μ -superoxo) complex at low temperature, and its thermal decomposition leads to the dinuclear $\text{Co(II)}-\mu\text{-peroxo}$ species $\{\text{Co}[\text{HB(3-Pr}^i\text{-5-Mepz)}_3]\}_2(\mu\text{-O}_2)$.^{13b,c} Although further decomposition of the $\text{Co(II)}-\mu\text{-peroxo}$ species induces dehydrogenation of the proximal pyrazole substituent (Pr^i) giving the isopropenyl group, O-atom transfer to an organic substrate is not observed.^{13b}

Many examples of the ligand oxygenation have been explained in terms of putative MOOX ($\text{X} = \text{metal, none, H, alkyl, acyl}$) species. However, the aliphatic C-H bond oxygenation is rare^{9a,11d,14} compared to the aromatic oxygenation,^{8e,15,16} and only a few MOOX intermediates which induce O-O and C-H bond activation have been characterized. Here we report the intramolecular aliphatic C-H bond oxygenation induced by the spontaneous decomposition of $\text{Co(II)}-\text{peroxo}^5$ species $\{\text{Co}[\text{HB(3,5-Pr}^i_2\text{pz)}_3]\}_2(\mu\text{-O}_2)$ and $\text{Co(OOR)}[\text{HB(3,5-Pr}^i_2\text{pz)}_3]$, which are yielded by the reaction of $\{\text{Co}(\mu\text{-OH)}[\text{HB(3,5-Pr}^i_2\text{pz)}_3]\}_2$ with ROOH ($\text{R} = \text{H, alkyl}$). The first structural determination of the $\text{Co(II)}-\text{alkylperoxo}$ complex stabilized by the sterically demanding $\text{HB(3-Bu}^t\text{-5-Pr}^i\text{pz)}_3$ ligand is also reported.

Experimental Section

Instrumentation. ^1H NMR spectra were recorded on a JEOL-GX-270 spectrometer (270 MHz for ^1H). The chemical shifts are reported as values (δ , ppm) downshifted from the internal standard Me_4Si . IR measurements were carried out as KBr pellets using a JASCO FT/IR-5300 instrument. Electronic spectra were recorded on a Shimadzu UV-260 spectrometer. Low-temperature electronic spectra were obtained using an Oxford DN1704 cryostat. Field desorption mass spectra were recorded on a Hitachi M-80 mass spectrometer. The X-ray data collections were performed on Rigaku four-circle AFC-5S and AFC-5R diffractometers. The X-ray data analysis was completed by the TEXSAN structure solving program system on an Indigo-IRIS computer (Silicon Graphics), obtained from Rigaku.

Materials and Methods. All solvents used were purified by the literature methods.¹⁷ The reagents of the highest grade commercially available were used without further purification. All manipulations were performed under argon by standard Schlenk techniques. The dinuclear $\text{Co(II)}-\text{bis}(\mu\text{-hydroxo})$ complex $\{\text{Co}(\mu\text{-OH)}[\text{HB(3,5-Pr}^i_2\text{pz)}_3]\}_2$ (1),¹⁸ $\{\text{Co}[\text{HB(3,5-Pr}^i_2\text{pz)}_3]\}_2(\mu\text{-O}_2)$ (2),¹⁹ and the potassium salt of

(8) Fe complexes: (a) Kitajima, N.; Fukui, H.; Moro-oka, Y.; Mizutani, Y.; Kitagawa, T. *J. Am. Chem. Soc.* **1990**, *112*, 6402. (b) Kitajima, N.; Tamura, N.; Amagai, H.; Fukui, H.; Moro-oka, Y.; Mizutani, Y.; Kitagawa, T.; Mathur, R.; Heerwegh, K.; Reed, C. A.; Randall, C. R.; Que, L., Jr.; Tatum, K. *J. Am. Chem. Soc.* **1994**, *116*, 9071. (c) Kitajima, N.; Tamura, N.; Tanaka, M.; Moro-oka, Y. *Inorg. Chem.* **1992**, *31*, 3342. (d) Kitajima, N.; Amagai, H.; Tamura, N.; Ito, M.; Moro-oka, Y.; Heerwegh, K.; Pénicaud, A.; Mathur, R.; Reed, C. A.; Boyd, P. D. W. *Inorg. Chem.* **1993**, *32*, 3583. (e) Kitajima, N.; Ito, M.; Fukui, H.; Moro-oka, Y. *J. Am. Chem. Soc.* **1993**, *115*, 9335. (f) Ito, M.; Amagai, H.; Fukui, H.; Kitajima, N.; Moro-oka, Y. *Bull. Chem. Soc. Jpn.* **1996**, *69*, 1937. The molecular structure of the dinuclear $\text{Fe(III)}-\mu\text{-1,2-peroxobis}(\mu\text{-carboxylato})$ complex bearing the $\text{HB(3,5-Pr}^i_2\text{pz)}_3$ ligand has been reported by Kim and Lippard: Kim, K.; Lippard, S. J. *J. Am. Chem. Soc.* **1996**, *118*, 4914.

(9) Mn complexes: (a) Kitajima, N.; Osawa, M.; Tanaka, M.; Moro-oka, Y. *J. Am. Chem. Soc.* **1991**, *113*, 8952. (b) Kitajima, N.; Osawa, M.; Tamura, N.; Moro-oka, Y.; Hirano, T.; Hirobe, M.; Nagano, T. *Inorg. Chem.* **1993**, *32*, 1879. (c) Kitajima, N.; Komatsuzaki, H.; Hikichi, S.; Osawa, M.; Moro-oka, Y. *J. Am. Chem. Soc.* **1994**, *116*, 11596.

(10) (a) Solomon, E. I.; Tuzcek, F.; Root, D. E.; Brown, C. A. *Chem. Rev.* **1994**, *94*, 827. (b) Baldwin, M. J.; Root, D. E.; Pate, J. E.; Fujisawa, K.; Kitajima, N.; Solomon, E. I. *J. Am. Chem. Soc.* **1992**, *114*, 10421. (c) Ross, P. K.; Solomon, E. I. *J. Am. Chem. Soc.* **1990**, *112*, 5871. (d) Ross, P. K.; Solomon, E. I. *J. Am. Chem. Soc.* **1991**, *113*, 3246.

(11) (a) Mahapatra, S.; Halfen, J. A.; Wilkinson, E. C.; Pan, G.; Cramer, C. J.; Que, L., Jr.; Tolman, W. B. *J. Am. Chem. Soc.* **1995**, *117*, 8865. (b) Halfen, J. A.; Mahapatra, S.; Wilkinson, E. C.; Kaderli, S.; Young, V. G., Jr.; Que, L., Jr.; Zuberbühler, A. D.; Tolman, W. B. *Science* **1996**, *271*, 1397. (c) Mahapatra, S.; Halfen, J. A.; Wilkinson, E. C.; Pan, G.; Wang, X.; Young, V. G., Jr.; Cramer, C. J.; Que, L., Jr.; Tolman, W. B. *J. Am. Chem. Soc.* **1996**, *118*, 11555. (d) Mahapatra, S.; Halfen, J. A.; Tolman, W. B. *J. Am. Chem. Soc.* **1996**, *118*, 11575. (e) Mahapatra, S.; Young, V. G., Jr.; Kaderli, S.; Zuberbühler, A. D.; Tolman, W. B. *Angew. Chem., Int. Ed. Engl.* **1997**, *36*, 130. (f) Tolman, W. B. *Acc. Chem. Res.* **1997**, *30*, 227.

(12) (a) Giannotti, C.; Fontaine, C.; Chiaroni, A.; Riche, C. *J. Organomet. Chem.* **1976**, *113*, 57. (b) Nishinaga, A.; Tomita, H.; Nishizawa, K.; Matsuura, T.; Ooi, S.; Hirotsu, K. *J. Chem. Soc., Dalton Trans.* **1981**, 1504. (c) Saussine, L.; Brazis, E.; Robine, A.; Mimoun, H.; Fischer, J.; Weiss, R. *J. Am. Chem. Soc.* **1985**, *107*, 3534. (d) Chavez, F. A.; Nguyen, C. V.; Olmstead, M. M.; Mascharak, P. K. *Inorg. Chem.* **1996**, *35*, 6282.

(13) (a) Egan, J. W., Jr.; Haggerty, B. S.; Rheingold, A. L.; Sendlinger, S. C.; Theopold, K. H. *J. Am. Chem. Soc.* **1990**, *112*, 2445. (b) Reinaud, O. M.; Theopold, K. H. *J. Am. Chem. Soc.* **1994**, *116*, 6979. (c) Reinaud, O. M.; Yap, G. P. A.; Rheingold, A. L.; Theopold, K. H. *Angew. Chem., Int. Ed. Engl.* **1995**, *34*, 2051.

(14) (a) Day, V. W.; Klemperer, W. G.; Lockledge, S. P.; Main, D. J. *J. Am. Chem. Soc.* **1990**, *112*, 2031. (b) Chen, D.; Martell, A. E. *J. Am. Chem. Soc.* **1990**, *112*, 9411. (c) Sanyal, I.; Mahroof-Tahir, M.; Nasir, M. S.; Ghosh, P.; Cohen, B. I.; Gultneh, Y.; Cruse, R. W.; Farooq, A.; Karlin, K. D.; Liu, S.; Zubieta, J. *Inorg. Chem.* **1992**, *31*, 4322. (d) Itoh, S.; Kondo, T.; Komatsu, M.; Ohshiro, Y.; Li, C.; Kanehisa, N.; Kai, Y.; Fukuzumi, S. *J. Am. Chem. Soc.* **1995**, *117*, 4714. (e) Halfen, J. A.; Young, V. G., Jr.; Tolman, W. B. *J. Am. Chem. Soc.* **1996**, *118*, 10920. (f) Allen, W. E.; Sorrell, T. N. *Inorg. Chem.* **1997**, *36*, 1732.

(15) (a) Karlin, K. D.; Dahlstrom, P. L.; Cozzette, S. N.; Scensny, P. M.; Zubieta, J. *J. Chem. Soc., Chem. Commun.* **1981**, 881. (b) Karlin, K. D.; Hayes, J. C.; Gultneh, Y.; Cruse, R. W.; McKown, J. W.; Hutchinson, J. P.; Zubieta, J. *J. Am. Chem. Soc.* **1984**, *106*, 2121. (c) Nasir, M. S.; Karlin, K. D.; McGowty, D.; Zubieta, J. *J. Am. Chem. Soc.* **1991**, *113*, 698. (d) Nasir, M. S.; Cohen, B. I.; Karlin, K. D. *J. Am. Chem. Soc.* **1992**, *114*, 2482. (e) Karlin, K. D.; Kaderli, S.; Zuberbühler, A. D. *Acc. Chem. Res.* **1997**, *30*, 139. (f) Menif, R.; Martell, A. E. *J. Chem. Soc., Chem. Commun.* **1989**, 1521. (g) Menif, R.; Martell, A. E.; Squattrito, P. J.; Clearfield, A. *Inorg. Chem.* **1990**, *29*, 4723. (h) Casella, L.; Rigoni, L. *J. Chem. Soc., Chem. Commun.* **1985**, 1668. (i) Casella, L.; Gullotti, M.; Pallanza, G.; Rigoni, L. *J. Am. Chem. Soc.* **1988**, *110*, 4221. (j) Sorrell, T. N.; Vankai, V. A.; Garrity, M. L. *Inorg. Chem.* **1991**, *30*, 207.

(16) Ménage, S.; Galey, J.-B.; Hussler, G.; Seitö, M.; Fontecave, M. *Angew. Chem., Int. Ed. Engl.* **1996**, *35*, 2353.

(17) Perrin, D. D.; Armarego, W. L.; Perrin, D. R. *Purification of Laboratory Chemicals*, 2nd ed.; Pergamon: New York, 1980.

(18) Kitajima, N.; Hikichi, S.; Tanaka, M.; Moro-oka, Y. *J. Am. Chem. Soc.* **1993**, *115*, 5496.

(19) Hikichi, S.; Komatsuzaki, H.; Kitajima, N.; Akita, M.; Mukai, M.; Kitagawa, T.; Moro-oka, Y. *Inorg. Chem.* **1997**, *36*, 266.

hydrotris(3-*tert*-butyl-5-isopropylpyrazol-1-yl)borate²⁰ were prepared by the method described previously.

Thermal Decomposition of the μ -Peroxo Complex 2 Giving

$\text{Co}_2(\mu\text{-OH})[\text{HB}(\mu\text{-3-OCMe}_2\text{-5-Pr}^i\text{pz})(3,5\text{-Pr}^i\text{pz})_2][\text{HB}(3,5\text{-Pr}^i\text{pz})_3]$ (**4**). When a 10-mL pentane solution of **2** (35.0 mg, 0.032 mmol) was left at room temperature, the solution color changed from dark brown to dark red within 30 min. From this solution, red crystals of bis(μ -hydroxo) complex **1** were isolated by cooling at -20°C (14.7 mg, 0.014 mmol, 42% yield). After removal of **1**, the filtrate was evaporated and the resulting dark red solid was dissolved in MeCN. Upon recrystallization from the MeCN solution, brownish red compound **4** was obtained as a crystalline solid (3.9 mg, 0.004 mmol, 11% yield). Anal. Calcd for $\text{C}_{54}\text{H}_{92}\text{N}_{12}\text{O}_2\text{B}_2\text{Co}_2$: C, 60.01; H, 8.58; N, 15.41. Found: C, 59.74; H, 8.52; N, 15.41. IR (KBr pellet, ν/cm^{-1}): 3712 (OH), 2529 (BH), 1260 (CO). UV–vis (toluene, room temperature, nm, $\epsilon/\text{M}^{-1}\text{cm}^{-1}$): 440 (sh), 492 (115), 535 (sh), 660 (35), 740 (40). FD-MS (m/z): 1080 (**4**⁺, 100%), 1108 (**4**⁺ + CO, 67%), 1124 (**4**⁺ + CO₂, 5%).

Reaction of Bis(μ -Hydroxo) Complex 1 with Excess H₂O₂ Giving

$\{\text{Co}[\text{HB}(\mu\text{-3-OCMe}_2\text{-5-Pr}^i\text{pz})(3,5\text{-Pr}^i\text{pz})_2]\}_2$ (**5**) and $\text{Co}(\text{OH})[\text{HB}(3\text{-Me}_2\text{COH-5-Pr}^i\text{pz})(3\text{-Me}_2\text{COH-5-Pr}^i\text{pz})_2](\text{H}_2\text{O})$ (**6**). When 10 equiv of aqueous 35 wt % H₂O₂ (0.65 mL, 6.69 mmol) was added dropwise to a toluene solution (10 mL) of **1** (727.0 mg, 0.672 mmol) at -78°C , the red solution changed to a dark brown one. UV–vis spectrum of this brown solution was identical with that of a toluene solution of the isolated sample of **2**. After being stirred for 2 h at -78°C , the reaction mixture was slowly warmed to room temperature and stirring was continued for 12 h. The resulting heterogeneous mixture was washed with water, and evaporation of the organic layer gave brown solids. Recrystallization from MeCN solution afforded deep blue-green crystals **5** (326 mg, 0.302 mmol, 45% yield). The filtrate of **5** was concentrated, and standing at room temperature under argon afforded **6** as pale brown crystals (87.1 mg, 0.148 mmol, 11% yield).

Spectroscopic data for **5**: Anal. Calcd for $\text{C}_{56}\text{H}_{93}\text{N}_{13}\text{O}_2\text{B}_2\text{Co}_2$ (**5**·MeCN): C, 60.06; H, 8.37; N, 16.26. Found: C, 59.63; H, 8.62; N, 16.01. IR (KBr pellet, ν/cm^{-1}): 2532 (BH), 1260 (CO). UV–vis (toluene, 23 $^\circ\text{C}$, nm, $\epsilon/\text{M}^{-1}\text{cm}^{-1}$): 448 (130), 480 (sh, 90), 582 (95), 605 (sh, 80), 791 (40). FD-MS (m/z): 1078 (**5**⁺, 100%). μ_{eff} ($\mu_{\text{B}}/\text{mol}$): 7.52 (5.32 μ_{B}/Co).

Spectroscopic data for **6**: Anal. Calcd for $\text{C}_{27}\text{H}_{47}\text{N}_6\text{O}_4\text{BCo}$ (**6**): C, 55.02; H, 8.04; N, 14.62. Found: C, 54.73; H, 8.15; N, 14.29. IR (KBr pellet, ν/cm^{-1}): 3363 (s, br, OH), 2533 (BH), 1222 (CO). UV–vis (toluene, 23 $^\circ\text{C}$, nm, $\epsilon/\text{M}^{-1}\text{cm}^{-1}$): 434 (200), 494 (175), 550 (150), 620 (sh, 85), 680 (sh, 65), 720 (sh, 40). FD-MS (m/z): 571 (**6**⁺ – H₂O, 100%), 554 (**6**⁺ – H₂O – OH, 20%). μ_{eff} ($\mu_{\text{B}}/\text{mol}$): 4.88.

Reaction of 5 with H₂O₂ Giving 6. Aqueous H₂O₂ (0.1 mL, 1.03 mmol, 35 wt %) was added dropwise to an acetone solution (20 mL) of **5** (101.1 mg, 0.0904 mmol) at -78°C . The reaction mixture was slowly warmed to room temperature and stirred for 24 h. After removal of the solvent under vacuum, the resulting solid was dissolved in MeCN. Crystallization at room temperature under argon afforded the unreacted **5**, and it was removed by filtration. The pale brown crystals of **6** was obtained from the concentrated filtrate (18.8 mg, 0.0319 mmol, 18% yield).

Reaction of Bis(μ -hydroxo) Complex 1 with ROOH (Formation of 5 via $\text{Co}(\text{OOR})[\text{HB}(3,5\text{-Pr}^i\text{pz})_3]$ (3a**; R = Bu^t, **3b**; R = PhMe₂C)).** When 2 equiv of Bu^tOOH (80%, 25 mL, 0.20 mmol) was added to a cold (-78°C) pentane solution of **1** (102.6 mg, 0.0947 mmol) in 15 mL of pentane, the red solution changed immediately to a blue one. Stirring of the solution was continued for 2 h at -78°C , and the solution color turned from blue to dark brownish green. The solvent was evaporated under vacuum at room temperature, then recrystallization of the resulting solid from MeCN afforded the blueish green crystalline solid of **5** (38.8 mg, 0.0360 mmol, 38% yield based on **1**). After removal of **5**, the filtrate was evaporated under vacuum. An IR spectrum of the resulting solid contained the peak at 3712 cm^{-1} arising

from the bis(μ -hydroxo) complex **1**. Reaction of **1** with PhMe₂COOH performed under the same conditions also yielded **5** (32% yield).

Co(OAc)[HB(3-Bu^t-5-Prⁱpz)₃] (7**).** A MeOH solution (15 mL) of Co(OAc)₂ (0.52 g, 2.09 mmol) was added to a THF solution (20 mL) of K[HB(3-Bu^t-5-Prⁱpz)₃] (1.11 g, 2.03 mmol), and this reaction mixture was stirred for 15 min. After removal of the solvent under vacuum, the product was extracted from the residue with 30 mL of toluene and the toluene phase was evaporated under vacuum. The resulting bluish purple solid was recrystallized from MeCN at -20°C (0.91 g, 1.46 mmol, 72% yield). Anal. Calcd for $\text{C}_{32}\text{H}_{55}\text{N}_6\text{O}_2\text{BCo}$: C, 61.44; H, 8.86; N, 13.43. Found: C, 61.27; H, 8.67; N, 13.62. IR (KBr pellet, ν/cm^{-1}): 2566 (BH), 1575 (br, COOas). FD-MS (m/z): 626 (**7**⁺, 100%).

Co(OH)[HB(3-Bu^t-5-Prⁱpz)₃] (8**).** A toluene solution (20 mL) of **7** (212 mg, 0.338 mmol) was treated with 5 mL of 1 M aqueous NaOH for 10 min under argon. The toluene phase was separated and dried under vacuum. The resulting deep blue solid was dissolved in MeCN, and crystallization at -20°C afforded **8** as microcrystalline blue solid (116 mg, 0.200 mmol, 59% yield). Anal. Calcd for $\text{C}_{30}\text{H}_{53}\text{N}_6\text{OBCo}$: C, 61.74; H, 9.15; N, 14.40. Found: C, 61.83; H, 9.10; N, 14.06. IR (KBr pellet, ν/cm^{-1}): 3670 (OH), 2553 (BH). FD-MS (m/z): 1193 (**8** + CO₂ – H₂O, 100%), 567 (**8** – OH, 43%).

Co(OOCMePh)[HB(3-Bu^t-5-Prⁱpz)₃] (9**).** The mononuclear Co(II)–hydroxo complex **8** (43.7 mg, 0.0749 mmol) was stirred with 1.2 equiv of cumyl hydroperoxide (80 wt %, 20 mL, 0.09 mmol) in CH₂Cl₂ (10 mL) for 30 min at -50°C . After removal of the solvent under vacuum, the resulting deep blue solid was dissolved in a mixture of MeCN and Et₂O. Crystallization at -40°C yielded **9** as blue crystals (18.8 mg, 0.0262 mmol, 38% yield). Anal. Calcd for $\text{C}_{41}\text{H}_{66}\text{N}_7\text{O}_2\text{BCo}$ (**9**·MeCN): C, 64.90; H, 8.77; N, 12.92. Found: C, 64.92; H, 9.02; N, 12.58. IR (KBr pellet, ν/cm^{-1}): 2558 (BH). UV–vis (CH₂Cl₂, -78°C , nm, $\epsilon/\text{M}^{-1}\text{cm}^{-1}$): 350 (sh, 280), 549 (370), 597 (590), 663 (1160).

X-ray Data Collections and Structural Determinations. Crystals suitable for X-ray analysis of **4**, **5**·MeCN, and **6**·2MeCN were obtained from MeCN solutions at room temperature under argon atmosphere. Single crystals of **9**·MeCN were obtained by recrystallization from MeCN/Et₂O at -40°C . The crystals were sealed in a thin-wall glass capillary to avoid the reaction with atmospheric CO₂ or loss of the MeCN molecules for crystallization. A Mo X-ray source equipped with a graphite monochromator (Mo K α , $\lambda = 0.710\text{ 680 \AA}$) was used. Automatic centering and least-squares routines were carried out for all the compounds with 25 reflections of $20^\circ < 2\theta < 25^\circ$ to determine the cell parameters. Data collections were completed with ω – 2θ (**5**·MeCN and **9**·MeCN) and ω scan (**4** and **6**·2MeCN).

The structures of the complexes were solved by the direct method (SAPI-91). Subsequent difference Fourier synthesis easily located all the non-hydrogen atoms, which were refined anisotropically. Neutral scattering factors were obtained from the standard source.²¹ All hydrogen atoms except those attached to the oxygen atoms in **4** and **6** were located at the calculated positions and were not refined ($d(\text{C–H}) = 0.95\text{ \AA}$ with the isotropic thermal factor of $U_{\text{iso}}(\text{H}) = 1.2U_{\text{iso}}(\text{C})$). The cell parameters, data collections, and refinement results are provided in Table 1. Full interatomic distances, bond angles, atomic coordinates, and isotropic and anisotropic thermal parameters are available as Supporting Information.

Results

Formation of Co(II)–Peroxo Complexes.⁵ Because low-spin d⁶ Co(III) compounds are kinetically inert, a large number of Co^{III}_{*n*}–OOR (*n* = 1, 2; R = none, H, alkyl) complexes have been isolated and characterized.^{1c,12} In general, such Co(III)–dioxygen complexes are yielded by oxidative addition of dioxygen to Co(II) complexes or chemical oxidation of Co(II) center by ROOH (R = H, alkyl) followed by complexation with a peroxo anion. We have reported that the dinuclear Co(II)–bis(μ -hydroxo) complex, $\{\text{Co}(\mu\text{-OH})[\text{HB}(3,5\text{-Pr}^i\text{pz})_3]\}_2$ (**1**), is basic enough to react with the atmospheric CO₂; however, **1** is unreactive toward dioxygen and never gives Co(III) com-

(20) Imai, S.; Fujisawa, K.; Kobayashi, T.; Shirasawa, N.; Fujii, H.; Yoshimura, T.; Kitajima, N.; Moro-oka, Y. Submitted for publication.

Table 1. Crystal Data and Data Collection Details of **4**, **5**·MeCN, **6**·2MeCN, and **9**·MeCN

	4	5 ·MeCN	6 ·2MeCN	9 ·MeCN
formula	C ₅₄ H ₉₂ N ₁₂ O ₂ B ₂ Co ₂	C ₅₆ H ₉₃ N ₁₃ O ₂ B ₂ Co ₂	C ₃₁ H ₅₃ N ₈ O ₄ BCo	C ₄₁ H ₆₆ N ₇ O ₂ BCo
formula weight	1080.89	1119.92	671.56	758.76
crystal system	monoclinic	monoclinic	monoclinic	triclinic
space group	<i>P</i> 2 ₁ / <i>a</i>	<i>P</i> 2 ₁ / <i>a</i>	<i>P</i> 2 ₁ / <i>n</i>	<i>P</i> 1
<i>a</i> /Å	33.779(7)	25.972(6)	35.321(6)	17.273(3)
<i>b</i> /Å	11.515(3)	12.272(3)	10.937(4)	19.096(6)
<i>c</i> /Å	16.433(4)	21.009(3)	9.421(2)	13.808(3)
α /deg	90	90	90	106.86(2)
β /deg	95.24(2)	108.08(2)	91.37(2)	90.01(2)
γ /deg	90	90	90	96.04(2)
<i>V</i> /Å ³	6365(5)	6365(4)	3638(1)	4332(3)
<i>Z</i>	4	4	4	4
<i>D</i> (calcd)/g·cm ⁻³	1.13	1.17	1.22	1.16
crystal size/mm	0.1 × 0.05 × 0.07	0.2 × 0.2 × 0.25	0.35 × 0.3 × 0.03	0.1 × 0.1 × 0.15
data collection temp/°C	23	-80	-70	-70
diffractometer	Rigaku AFC-5R	Rigaku AFC-5S	Rigaku AFC-5S	Rigaku AFC-5S
radiation		graphite-monochromated Mo K α	Mo K α (λ = 0.710 68 Å)	
μ (Mo K α)/cm ⁻¹	5.67	5.69	5.16	4.37
scan mode	ω	ω -2 θ	ω	ω -2 θ
scan width/deg	1.18 + 0.14 tan θ	1.30 + 0.14 tan θ	1.30 + 0.14 tan θ	1.30 + 0.14 tan θ
scan speed/deg·min ⁻¹	8	6	6	6
2 θ range (deg)	5-45	3-50	3-45	3-45
octant measured	$\pm h, -k, +l$	$\pm h, +k, +l$	$\pm h, +k, +l$	$\pm h, \pm k, +l$
no. of measd reflections	9392	12071	7178	11969
no. of obsd reflections	3973 (<i>I</i> > 1.8 σ (<i>I</i>))	5501 (<i>I</i> > 3 σ (<i>I</i>))	4067 (<i>I</i> > 3 σ (<i>I</i>))	6031 (<i>I</i> > 2.5 σ (<i>I</i>))
no. of parameters refined	649	676	406	937
<i>R</i> /%	6.79	4.94	8.05	8.79
<i>R</i> _w /%	6.01	4.26	7.73	7.94

pounds.¹⁸ In addition, the first Co(II)-dioxygen compound is Co(II)-superoxo complex, not Co(III)-peroxo complex, with the similar hydrotris(pyrazolyl)borate ligand as mentioned in the Introduction.^{13a} Therefore, reaction of the Co(II)-bis(μ -hydroxo) complex **1** with stoichiometric amount of ROOH is expected to yield dimeric Co(II)- μ -peroxo and monomeric Co(II)-alkylperoxo complexes as found for the analogous Cu(II) complexes (Scheme 1).^{7d-f}

(a) Formation of the μ -Peroxo Complex 2. Reaction of the bis(μ -hydroxo) complex **1** with an equimolar amount of H₂O₂ at -50 °C afforded a dark brown compound **2**. This thermally unstable compound was identified as a dinuclear Co(II)- μ - η^2 : η^2 -peroxo complex, {Co[HB(3,5-Pr^{*i*}pz)₃]₂(μ -O₂)}, on the basis of its unique characteristics as reported previously.¹⁹

(b) Formation of the Alkylperoxo Complexes 3. Treatment of a pentane solution of the hydroxo complex **1** with 2 equiv of alkyl hydroperoxide (*tert*-butyl and cumyl hydroperoxides) at -78 °C gave a blue solution with an intense absorption around 650 nm, which was known as a characteristic feature of the high-spin Co(II) ion located in a tetrahedral ligand field. Although isolation of **3** was unsuccessful because of their thermal instability, they were identified as a tetrahedral Co(II) alkylperoxo compound, Co(OOR)[HB(3,5-Pr^{*i*}pz)₃] (**3a**; R = Bu^{*t*}, **3b**; R = PhMe₂C), by comparison with the isolated analogue **9** (see below).

Thermal Decomposition of Co(II)-Peroxo Complexes. The Co(II)-dioxygen complexes **2** and **3** were thermally unstable compared to the copper μ -peroxo and alkylperoxo complexes. The spontaneous decomposition of these Co(II)-peroxo species resulted in the oxygenation of the isopropyl substituents on the pyrazolyl ligands and the different decomposition products were obtained from **2** depending on the conditions (in the absence or the presence of H₂O₂) (Scheme 1). Formation of the mono-oxygenated compound **4** was reported earlier as a Communication.¹⁹

(1) Decomposition of the μ -Peroxo Complex 2. (a) In the Absence of H₂O₂. Spontaneous decomposition of **2** resulted

in the intramolecular oxygenation at one of the six isopropyl groups which were proximal to the Co centers. Dark brown color of a pentane solution of **2** was changed to dark red within 30 min at room temperature. Cooling to -20 °C followed by concentration of this solution allowed the isolation of **1**. After removal of **1**, the filtrate was evaporated and recrystallization from a MeCN solution of the resulting solid gave a brownish red complex **4** as crystalline solid. An IR spectrum of **4** exhibited a ν (O-H) band at 3712 cm⁻¹, which was clearly different from that of **1** (3700 cm⁻¹). X-ray crystallography revealed the unique structure of **4**, described as the μ -alkoxo- μ -hydroxo dinuclear Co(II) complex, Co₂(μ -OH)[HB(μ -3-OCMe₂-5-Pr^{*i*}pz)(3,5-Pr^{*i*}pz)₂][HB(3,5-Pr^{*i*}pz)₃] (Figure 1 and Table 2), in which one of the six methine groups in the isopropyl substituents proximal to the metal centers is oxygenated and the resulting alkoxide functional group bridges the two Co(II) centers. In addition, the five-membered ring formed by the bridging chelation caused distortion of the dinuclear metal core. The Co...Co separation of **4** is 3.078(2) Å, which is slightly shorter than those found in the bis(μ -hydroxo) core of **1** (3.202(3) and 3.189(3) Å).¹⁸ The Co1-O11(alkoxo)-Co2 angle (97.8(3)°) is smaller than the Co-O(hydroxo)-Co angles in **4** and **1** (101.9(3)° for **4**; 105.0(3)° and 105.5(3)° for **1**). The geometries of the Co ions in **4** are clearly different from the slightly distorted square pyramidal one of the bis(μ -hydroxo) complex **1**.¹⁸ Co1 has a highly distorted geometry, which is closer to trigonal bipyramid rather than square pyramid. The geometry of Co2 is best described as distorted trigonal bipyramid with the O11-Co2-N41 axis (174.0(3)°). In accord with its non symmetrical structure, a toluene-*d*₈ solution of **4** gives many paramagnetic-shifted ligand proton signals in the region -120 to +145 ppm. The non-symmetrical structure shows the complicated features in the visible spectrum of **4** compared with that of the symmetrical dinuclear complex such as **1**.

Scheme 1

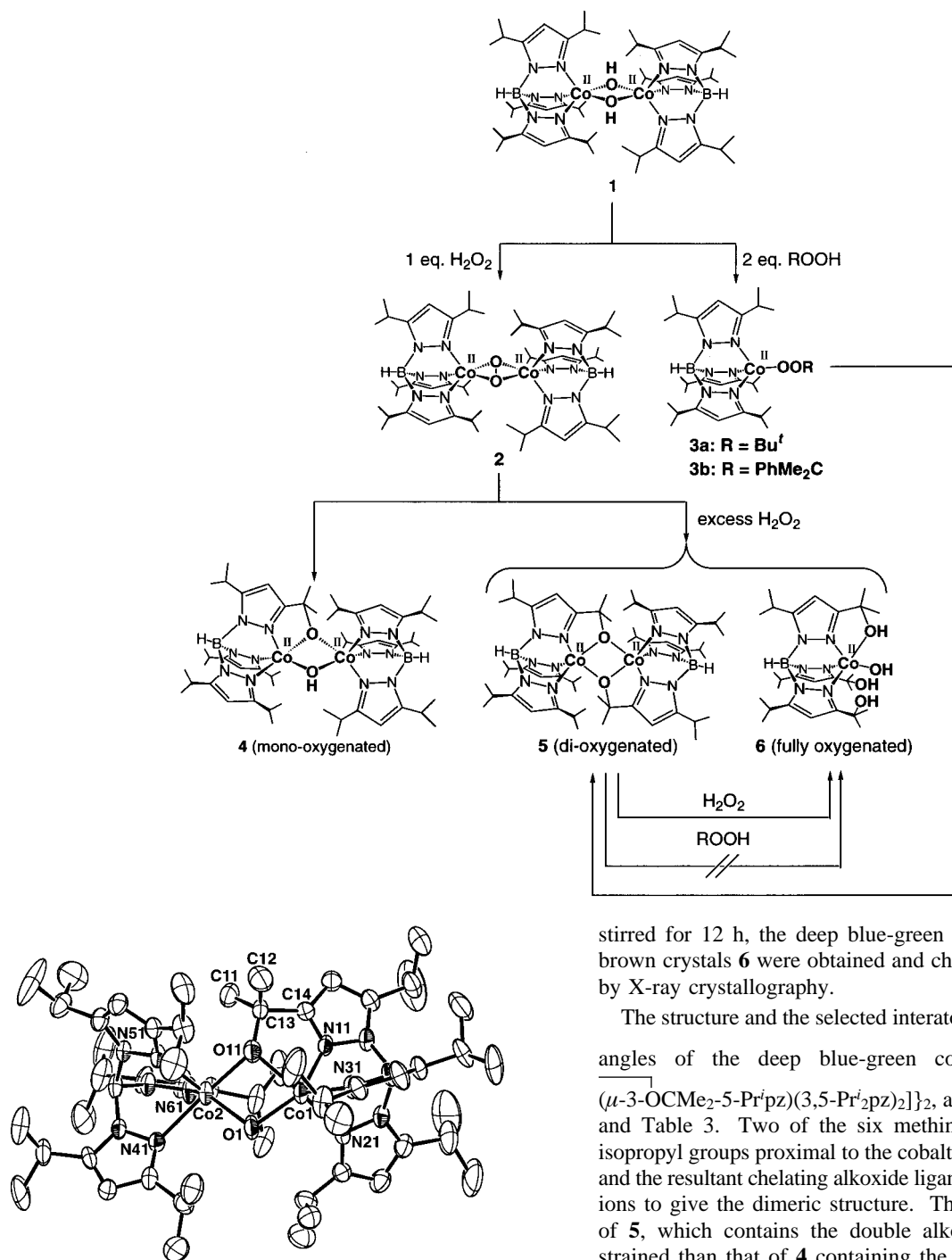


Figure 1. ORTEP drawing of $\text{Co}_2(\mu\text{-OH})[\text{HB}(\mu\text{-}3\text{-OCMe}_2\text{-}5\text{-Pr}^i\text{pz})\text{-}(3,5\text{-Pr}^i\text{pz}_2)_2][\text{HB}(3,5\text{-Pr}^i\text{pz}_3)]$ (**4**) (drawn at the 50% probability level). All hydrogen atoms are omitted for clarity.

The dinuclear core was found to be rigid because the bis(μ -alkoxo) complex **5** (see below) resulting from the redistribution of the Co fragments was not detected.

(b) In the Presence of an Excess Amount of H_2O_2 . Decomposition of **2** in the presence of an excess amount of H_2O_2 resulted in the formation of a mixture of two further oxygenated products. When 10 equiv of aqueous H_2O_2 was added to a toluene solution of **1** at -78°C , the red solution changed to a dark brown one, indicating the formation of μ -peroxo complex **2**. When the resulting mixture was warmed to room temperature without removal of the excess H_2O_2 and

stirred for 12 h, the deep blue-green crystals **5** and the pale brown crystals **6** were obtained and characterized successfully by X-ray crystallography.

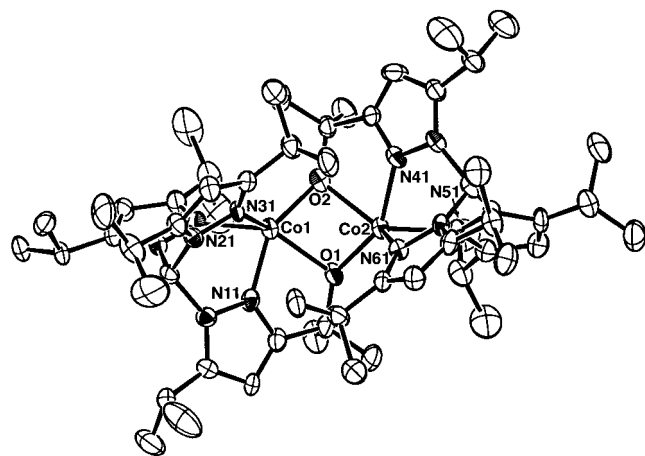
The structure and the selected interatomic distances and bond angles of the deep blue-green compound **5**, $\{\text{Co}[\text{HB}(\mu\text{-}3\text{-OCMe}_2\text{-}5\text{-Pr}^i\text{pz})(3,5\text{-Pr}^i\text{pz}_2)]_2\}_2$, are presented in Figure 2 and Table 3. Two of the six methine carbon atoms in the isopropyl groups proximal to the cobalt centers are oxygenated, and the resultant chelating alkoxide ligands bridge the two Co(II) ions to give the dimeric structure. The dinuclear Co(II) core of **5**, which contains the double alkoxide bridges, is more strained than that of **4** containing the single alkoxide bridge; the Co1–Co2 distance of **5** (2.944(1) Å) is shorter than that of **4**, and the Co1–O(alkoxide)–Co2 angles (91.2(2) and 91.4(2)°) are also more acute than that found in **4**. The geometries of the both Co(II) ions are best described as highly distorted trigonal bipyramid rather than square pyramid. The ^1H NMR spectrum of **5** also revealed the loss of the 3-fold symmetry of the tris(pyrazolyl)borate ligand arising from the oxygenation; many paramagnetically shifted signals were observed in the very wide range (-150 to $+110$ ppm).

In contrast to the structures of **4** and **5**, the pale brown compound **6** is monomeric as shown in Figure 3 (selected interatomic distances and bond angles are summarized in Table 4). The most striking structural feature is that all the proximal methine sites of the Pr^i groups are hydroxylated to give the chelating alcohol ligand and two free alcohol functional groups.

Table 2. Selected Interatomic Distances (Å) and Bond Angles (deg) for $\text{Co}_2(\mu\text{-OH})[\text{HB}(\mu\text{-}3\text{-OCMe}_2\text{-}5\text{-Pr}^i\text{Pz})(3,5\text{-Pr}^i_2\text{Pz})_2][\text{HB}(3,5\text{-Pr}^i_2\text{Pz})_3]$ (**4**)

Interatomic Distances					
Co1—O1	1.974(6)	Co1—O11	2.067(6)	Co1—N11	2.001(8)
Co1—N21	2.137(8)	Co1—N31	2.087(7)	Co2—O1	1.990(6)
Co2—O11	2.017(7)	Co2—N41	2.210(8)	Co2—N51	2.067(7)
Co2—N61	2.063(7)	O11—C13	1.45(1)	Co1—Co2	3.078(2)
O1—O11	2.517(9)				

Bond Angles					
O1—Co1—O11	77.0(2)	O1—Co1—N11	148.2(3)		
O1—Co1—N21	105.9(3)	O1—Co1—N31	122.9(3)		
O11—Co1—N11	75.3(3)	O11—Co1—N21	143.2(3)		
O11—Co1—N31	27.0(3)	N11—Co1—N21	87.6(3)		
N11—Co1—N31	86.7(3)	N21—Co1—N31	83.1(3)		
O1—Co2—O11	77.8(2)	O1—Co2—N41	97.5(3)		
O1—Co2—N51	136.2(3)	O1—Co2—N61	126.6(3)		
O11—Co2—N41	174.0(3)	O11—Co2—N51	98.4(3)		
O11—Co2—N61	102.6(3)	N41—Co2—N51	82.2(3)		
N41—Co2—N61	83.2(3)	N51—Co2—N61	97.0(3)		
Co1—O1—Co2	101.9(3)	Co1—O11—Co2	97.8(3)		
Co1—O11—C13	120.3(5)	Co2—O11—C13	136.8(6)		
O11—C13—C11	113.5(9)	O11—C13—C12	110.1(10)		
O11—C13—C14	104.5(8)				

**Figure 2.** ORTEP drawing of $\{\text{Co}[\text{HB}(\mu\text{-}3\text{-OCMe}_2\text{-}5\text{-Pr}^i\text{pz})(3,5\text{-Pr}^i_2\text{pz})_2]\}_2\cdot\text{MeCN}$ (**5**·MeCN) (drawn at the 50% probability level). All hydrogen atoms and the MeCN molecule are omitted for clarity.

The resulting hydroxy- Pr^i group, bulkier than the Pr^i group, hinders formation of a dinuclear structure like **5**, and the fifth coordination site is occupied by a hydroxide to form the trigonal-bipyramidal structure with the N11—Co1—O1 axis, which is very similar to the half part of **5**. The slightly shorter Co—O1 distance (1.959(6) Å) appears to fall in the range of Co—OH distances; therefore, the oxygen donor (O1) is assigned to a OH ligand. The Co1—O11 distance (2.144(5) Å), which is longer than the other Co—O(alkoxo) distances of **4** (mean 2.042 Å) and **5** (mean 2.055 Å), suggests that the O11 is a neutral protonated alcoholic oxygen, not deprotonated alkoxide.²³ The oxidation state of the metal center is assigned as 2+ on the basis of the following observations: (1) the magnetic susceptibility of a solid sample (4.88 μ_B/mol) characteristic of a high-spin Co(II) species, (2) the Co—N(pyrazolyl) distances (mean 2.086 Å) are comparable to those found in **4** (mean 2.094 Å) and **5** (2.086 Å), and (3) the lack of a counterion in the unit cell. Thus the pale brown product **6** has been identified as the monomeric

(21) *International Tables for X-ray Crystallography*; Kynoch Press: Birmingham, U.K., 1975; Vol. 4.(22) Cotton, F. A.; Wilkinson, G. *Advanced Inorganic Chemistry*, 5th ed.; Wiley: New York, 1988.**Table 3.** Selected Interatomic Distances (Å) and Bond Angles (deg) for $\{\text{Co}[\text{HB}(\mu\text{-}3\text{-OCMe}_2\text{-}5\text{-Pr}^i\text{pz})(3,5\text{-Pr}^i_2\text{pz})_2]\}_2\cdot\text{MeCN}$ (**5**·MeCN)

Interatomic Distances					
Co1—O1	2.176(4)	Co1—O2	1.927(4)	Co1—N11	2.013(5)
Co1—N21	2.081(5)	Co1—N31	2.165(5)	Co2—O1	1.929(4)
Co2—O2	2.187(4)	Co2—N41	2.009(5)	Co2—N51	2.087(5)
Co2—N61	2.163(5)	O1—C13	1.415(7)	O2—C43	1.422(8)
Co1—Co2	2.944(1)	O1—O2	2.533(6)		

Bond Angles					
O1—Co1—O2	76.0(2)	O1—Co1—N11	73.3(2)		
O1—Co1—N21	130.6(2)	O1—Co1—N31	132.7(2)		
O2—Co1—N11	149.2(2)	O2—Co1—N21	118.4(2)		
O2—Co1—N31	112.6(2)	N11—Co1—N21	84.2(2)		
N11—Co1—N31	87.2(2)	N21—Co1—N31	87.9(2)		
O1—Co2—O2	75.7(2)	O1—Co2—N41	148.4(2)		
O1—Co2—N51	120.0(2)	O1—Co2—N61	111.7(2)		
O2—Co2—N41	73.0(2)	O2—Co2—N51	131.3(2)		
O2—Co2—N61	130.1(2)	N41—Co2—N51	84.4(2)		
N41—Co2—N61	86.3(2)	N51—Co2—N61	89.3(2)		
Co1—O1—Co2	91.4(2)	Co1—O2—Co2	91.2(2)		
Co1—O1—C13	117.8(4)	Co2—O1—C13	140.8(4)		
Co1—O2—C43	139.9(4)	Co2—O2—C43	119.0(3)		
O1—C13—C11	111.4(5)	O1—C13—C12	108.7(5)		
O1—C13—C14	107.0(5)	O2—C43—C41	108.4(5)		
O2—C43—C42	112.7(5)	O2—C43—C44	105.5(5)		

Co(II)—hydroxy alcohol complex $\text{Co}(\text{OH})[\text{HB}(3\text{-Me}_2\text{COH-}5\text{-Pr}^i\text{pz})(3\text{-Me}_2\text{COH-}5\text{-Pr}^i\text{pz})_2]$.²³ Another structural characteristic of **6** is the intra- and intermolecular interactions between the hydroxide and the alcohols (see Figure 3b: O1—O21, 2.804(8) Å; O1—O31, 2.720(9) Å; O1—O11 (intermolecular), 2.536(7) Å). In fact, an IR spectrum of the solid sample contained the very broad and intense O—H stretching vibration in the region 3700–3100 cm^{-1} . The ¹H NMR spectrum of **6** also contained many paramagnetically shifted peaks, suggesting that the chelation via the alcohol ligand was retained in solution. It is notable that the fully oxygenated compound **6** was also obtained by treatment of an isolated sample of **5** with H₂O₂. This observation suggested that **5** was a precursor of **6**.

(2) Decomposition of the Alkylperoxy Complexes **3**.

Alkylperoxy complexes $\text{Co}(\text{OOR})[\text{HB}(3,5\text{-Pr}^i_2\text{pz})_3]$ (**3a**, R = Bu^t; **3b**, R = CMe₂Ph), derived from **1** and ROOH, also decomposed to give the dioxygenated bis(μ -alkoxo) compound **5**. Within 2 h, the blue solution changed into brownish green one, from which the dimeric alkoxo complex **5** was isolated. However, it is noteworthy that the fully oxygenated compound **6** was never formed even in the presence of a large excess amount of ROOH. Reaction of **5** with ROOH also never yielded **6**, whereas **5** reacted with H₂O₂ to give **6** (see above). The pK_a values of ROOH (in H₂O, 25 °C) are as follows: H₂O₂, 11.58; PhMe₂COOH, 12.60; Bu^tOOH, 12.80.²⁴ The less acidic ROOH compared to H₂O₂ might make the ligand exchange of the Co—O—R moiety in **5** less favorable.

Isolation and Characterization of the Co(II)—Alkylperoxy Complex, $\text{Co}(\text{OOCMe}_2\text{Ph})[\text{HB}(3\text{-Bu}^t\text{-}5\text{-Pr}^i\text{pz})_3]$ (9**).** Although the structures and reactivities of several Co(III)—alkylperoxy compounds are reported,¹² no alkylperoxy complexes of Co(II) have been characterized so far. As mentioned above, the full characterization of the alkylperoxy complexes **3** was unsuccessful because of their instability even at -78 °C. Then we made attempts to isolate an alkylperoxy complex of

(23) Allen and Sorrell have reported the ligand hydroxylated Cu(II) complex containing the similar chelating alcohol ligand. See ref 14f.

(24) *Handbook of Organic Chemistry*; Dean, J. A., Ed.; McGraw-Hill: New York, 1987.

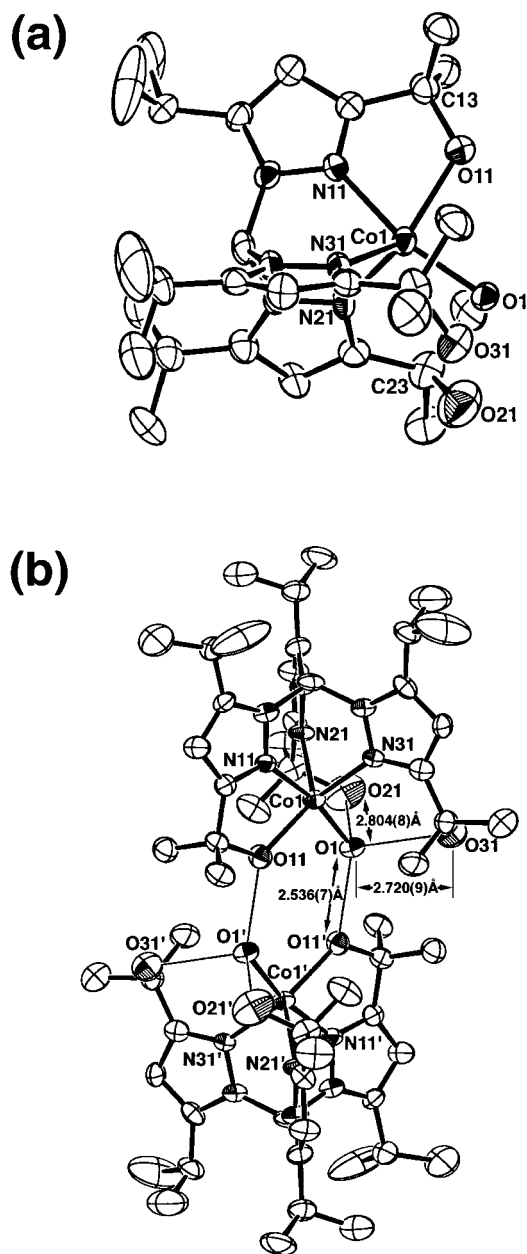


Figure 3. ORTEP drawing of $\text{Co}(\text{OH})[\text{HB}(3\text{-Me}_2\text{COH-5-Pr}'\text{pz})_2]\cdot 2\text{MeCN}$ ($6\cdot 2\text{MeCN}$) (drawn at the 50% probability level). All hydrogen atoms and the MeCN molecules are omitted for clarity: (a) molecular structure; (b) intra- and intermolecular contact of oxygen atoms.

Co(II) by using the sterically more hindered ligand hydrotris-(3-*tert*-butyl-5-isopropylpyrazol-1-yl)borate [$\text{HB}(3\text{-Bu}^t\text{-5-Pr}^i\text{-pz})_3$]. The $\text{HB}(3\text{-Bu}^t\text{-5-Pr}^i\text{-pz})_3$ ligand enforces formation of monomeric complexes arising from the sterical hindrance of *tert*-butyl substituents proximal to a metal center as found in the Cu^{25} and Fe^{26} complexes. The monomeric Co(II)–hydroxo complex, $\text{Co}(\text{OH})[\text{HB}(3\text{-Bu}^t\text{-5-Pr}^i\text{-pz})_3]$ (**8**), was prepared by treatment of the acetato complex, $\text{Co}(\text{OAc})[\text{HB}(3\text{-Bu}^t\text{-5-Pr}^i\text{-pz})_3]$ (**7**), with an aqueous NaOH solution. Reaction of **8** with 1 equiv of cumyl hydroperoxide at -40°C resulted in the formation of deep blue Co(II)–alkylperoxo complex, $\text{Co}(\text{OOCMe}_2\text{Ph})[\text{HB}(3\text{-Bu}^t\text{-5-Pr}^i\text{-pz})_3]$ (**9**) (Scheme 2). The structure of **9** was

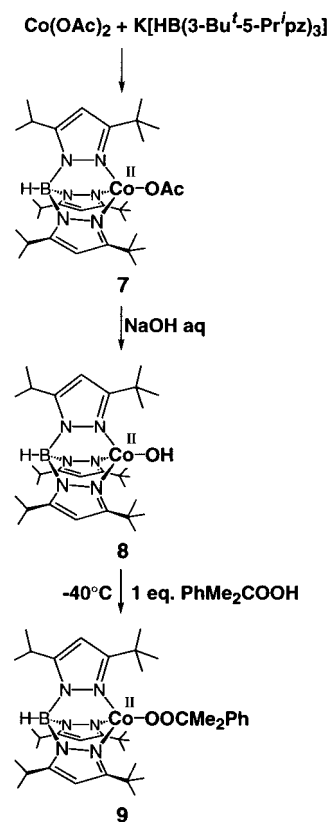
(25) Fujisawa, K.; Tanaka, M.; Moro-oka, Y.; Kitajima, N. *J. Am. Chem. Soc.* **1994**, *116*, 12079.

(26) Hikichi, S.; Ogihara, T.; Fujisawa, K.; Kitajima, N.; Akita, M.; Moro-oka, Y. *Inorg. Chem.* **1997**, *36*, 4539.

Table 4. Selected Interatomic Distances (Å) and Bond Angles (deg) for $\text{Co}(\text{OH})[\text{HB}(3\text{-Me}_2\text{COH-5-Pr}'\text{pz})_2]\cdot 2\text{MeCN}$ ($6\cdot 2\text{MeCN}$)

Interatomic Distances					
Co1–O1	1.958(5)	Co1–O11	2.144(5)	Co1–N11	2.025(6)
Co1–N21	2.122(6)	Co1–N31	2.104(6)	O11–C13	1.471(9)
O21–C23	1.50(1)	O31–C33	1.491(9)	O1–O21	2.804(8)
O1–O31	2.720(9)	O1–O11'	2.536(7)		
Bond Angles					
O1–Co1–O11	94.1(2)	O1–Co1–N11	167.4(2)		
O1–Co1–N21	104.9(2)	O1–Co1–N31	103.7(2)		
O11–Co1–N11	73.3(2)	O11–Co1–N21	129.7(2)		
O11–Co1–N31	132.1(2)	N11–Co1–N21	84.2(2)		
N11–Co1–N31	85.2(2)	N21–Co1–N31	88.2(2)		
Co1–O11–C13	120.1(4)	O11–C13–C11	109.0(7)		
O11–C13–C12	110.6(6)	O11–C13–C14	105.1(6)		
O21–C23–C21	108.5(7)	O21–C23–C22	104.0(8)		
O21–C23–C24	106.8(7)	O31–C33–C31	107.9(7)		
O31–C33–C32	104.3(8)	O31–C33–C34	109.7(6)		

Scheme 2



determined by X-ray crystallography as presented in Figure 4 and Table 5. A unit cell of **9** contained two crystallographically independent molecules with essentially the same structures. The lack of a counteranion in the unit cell implies that the oxidation state of metal center is 2+. The geometry of the Co(II) ions in **9** is best described as a slightly distorted tetrahedron coordinated by the oxygen atom of the end-on bound alkyl peroxide ligand and the three pyrazolyl nitrogen atoms. The shorter O–O distances (1.36(1) and 1.42(1) Å; mean 1.39 Å) compared to the O–O distances in the previously reported Co(III)–alkylperoxo complexes (1.42–1.52 Å)¹² may be attributed to the weaker Lewis acidity of the divalent cobalt ion, although the values of O–O lengths in **9** also fall in the typical range of the O–O bond lengths of the transition metal–alkylperoxo

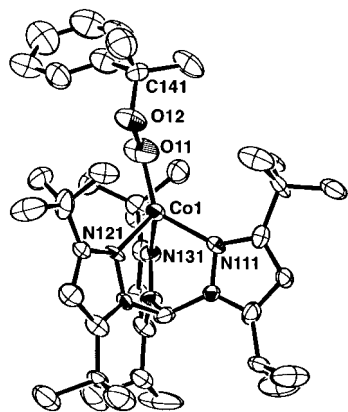


Figure 4. ORTEP drawing of $\text{Co}(\text{OOCMe}_2\text{Ph})[\text{HB}(3\text{-Bu}'\text{-}5\text{-Pr}'\text{pz})_3]\cdot\text{MeCN}$ (**9**·MeCN) (drawn at the 50% probability level). All hydrogen atoms and the MeCN molecules are omitted for clarity. One of crystallographically independent molecules is presented.

Table 5. Selected Bond Lengths (Å) and Bond Angles (deg) for $\text{Co}(\text{OOCMe}_2\text{Ph})[\text{HB}(3\text{-Bu}'\text{-}5\text{-Pr}'\text{pz})_3]\cdot\text{MeCN}$ (**9**·MeCN)

Molecule 1					
Bond Lengths					
Co1—O11	1.88(1)	Co1—N111	2.018(9)	Co1—N121	2.058(8)
Co1—N131	2.061(9)	O11—O12	1.36(1)	O12—C141	1.47(1)
Bond Angles					
O11—Co1—N111	133.1(4)	O11—Co1—N121	124.6(4)		
O11—Co1—N131	108.4(4)	N111—Co1—N121	93.9(3)		
N111—Co1—N131	89.8(3)	N121—Co1—N131	97.1(3)		
Co1—O11—O12	116.7(8)	O11—O12—C141	108(1)		
Molecule 2					
Bond Lengths					
Co2—O21	1.849(7)	Co2—N211	2.050(9)	Co2—N221	2.01(1)
Co2—N231	2.039(9)	O21—O22	1.42(1)	O22—C241	1.54(1)
Bond Angles					
O21—Co2—N211	112.5(4)	O21—Co2—N221	126.2(4)		
O21—Co2—N231	127.6(4)	N211—Co2—N221	93.1(4)		
N211—Co2—N231	91.7(3)	N221—Co2—N231	96.1(4)		
Co2—O21—O22	108.1(6)	O21—O22—C241	107.3(9)		

complexes.^{7f,27} Monomeric tetrahedral Co(II) complex **9** is the first example of a structurally characterized Co(II)—alkylperoxo complex.

The UV—vis spectra of CH_2Cl_2 solutions of **8** and **9** and a reaction mixture of **1** with 2 equiv of PhMe_2COOH in CH_2Cl_2 recorded at -78°C are presented in Figure 5. All of the three spectra show similar features; the very intense absorptions around 600 nm arise from the d—d transition of the tetrahedral Co(II) centers.²² This observation supports the identification

(27) (a) Boche, G.; Möbus, K.; Harms, K.; Marsch, M. *J. Am. Chem. Soc.* **1996**, *118*, 2770. (b) van Asselt, A.; Santarsiero, B. D.; Bercaw, J. E. *J. Am. Chem. Soc.* **1986**, *108*, 8291. (c) Mimoun, H.; Chaumette, P.; Mignard, M.; Saussine, L.; Fischer, J.; Weiss, R. *Nouv. J. Chim.* **1983**, *7*, 467. (d) Mimoun, H.; Charpentier, R.; Mitschler, A.; Fischer, J.; Weiss, R. *J. Am. Chem. Soc.* **1980**, *102*, 1047. (e) Ferguson, G.; Monaghan, P. K.; Parvez, M.; Puddephatt, R. J. *Organometallics* **1985**, *4*, 1669. (f) Strukul, G.; Michelin, R. A.; Orbell, J. D.; Randaccio, L. *Inorg. Chem.* **1983**, *22*, 3706. Several alkylperoxo complexes have been isolated; however, their structural characterizations have not been successful so far. (g) Zang, Y.; Elgren, T. E.; Dong, Y.; Que, L., Jr. *J. Am. Chem. Soc.* **1993**, *115*, 811. (h) Ménage, S.; Wilkinson, E. C.; Que, L., Jr.; Fontecave, M. *Angew. Chem., Int. Ed. Engl.* **1995**, *34*, 203. (i) Kim, J.; Larka, E.; Wilkinson, E. C.; Que, L., Jr. *Angew. Chem., Int. Ed. Engl.* **1995**, *34*, 2048. (j) Kim, J.; Dong, Y.; Larka, E.; Que, L., Jr. *Inorg. Chem.* **1996**, *35*, 2369. (k) Nguyen, C.; Guajardo, R. J.; Mascharak, P. K. *Inorg. Chem.* **1996**, *35*, 6273. (l) Zang, Y.; Kim, J.; Dong, Y.; Wilkinson, E. C.; Appelman, E. H.; Que, L., Jr. *J. Am. Chem. Soc.* **1997**, *119*, 4197. (m) Arasasingham, R. D.; Balch, A. L.; Cornman, C. R.; Latos-Grazynski, L. *J. Am. Chem. Soc.* **1989**, *111*, 4357. (n) Arasasingham, R. D.; Cornman, C. R.; Balch, A. L. *J. Am. Chem. Soc.* **1989**, *111*, 7800.

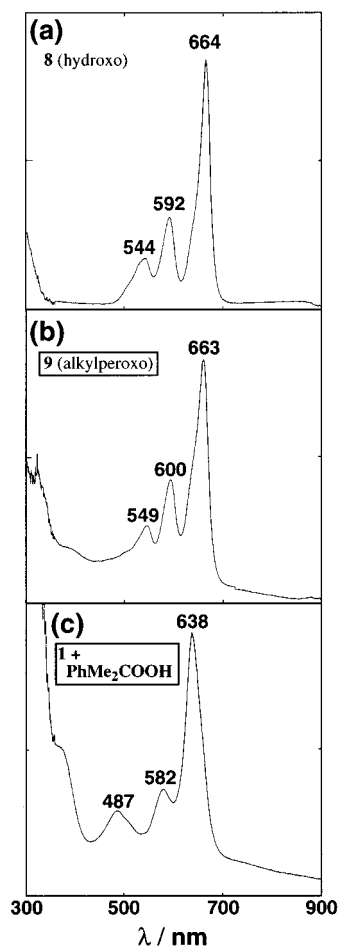


Figure 5. UV—vis spectra of **8** and **9**, and the reaction mixture of bis(μ -hydroxo)complex **1** with 2 equiv of cumyl hydroperoxide (in situ sample of **3b**). All spectra were recorded in CH_2Cl_2 solution at -78°C : (a) 1.43 mM CH_2Cl_2 solution of the monomeric hydroxo complex **8**; (b) 1.43 mM CH_2Cl_2 solution of the alkylperoxo complex of **9**; (c) 2 equiv of cumyl hydroperoxide added to a CH_2Cl_2 solution of **1** (4.81 mM) at -78°C .

of the unstable intermediate **3** as the Co(II)—alkylperoxo compounds (vide supra).

Discussion

The first-row transition metal—peroxo complexes⁵ having the $\text{HB}(3,5\text{-Pr}'_2\text{pz})_3$ ligand have been investigated as biomimetic models in our laboratory. The reaction of the Cu(II)—hydroxo complex, $\{\text{Cu}(\mu\text{-OH})[\text{HB}(3,5\text{-Pr}'_2\text{pz})_3]\}_2$, with ROOH (R = H, Bu', PhMe_2C , and $m\text{-Cl-C}_6\text{H}_4\text{C(O)}$) leads to the successful isolation and characterization of the Cu(II)— μ -peroxo,^{7d,e} —alkylperoxo,^{7f} and —acylperoxo^{7g} complexes. Although the alkylperoxo and acylperoxo complexes are capable of oxo transfer toward external substrates such as phosphine and sulfoxide, they exhibit no oxygenation activities toward hydrocarbons under anaerobic conditions. The Cu(II)₂— μ - η^2 : η^2 -peroxo complex, which can reproduce the spectroscopic characteristics of oxytyrosinase, is sluggish with respect to oxygenation. The first example of the intramolecular oxygenation of the hydrotris(pyrazolyl)borate ligand is observed in the manganese complex. The reaction of $\{\text{Mn}(\mu\text{-OH})[\text{HB}(3,5\text{-Pr}'_2\text{pz})_3]\}_2$ with O_2 results in the ligand oxygenated dinuclear Mn(III)— μ -oxo complex, $\{\text{Mn}[\text{HB}(3\text{-OCMe}_2\text{-}5\text{-Pr}'_2\text{pz})_3](3,5\text{-Pr}'_2\text{pz})_2\}_2(\mu\text{-O})$. This ligand oxygenation is presumed to proceed via Mn(III) μ -peroxo species; however, attempts to

isolate and characterize the Mn–dioxygen compounds have been unsuccessful so far.^{9a}

In this study, we have demonstrated the aliphatic C–H bond oxygenation via transition metal–peroxo⁵ species by isolation of the ligand oxygenated products. The present results, in particular the structure of the oxygenated products, give us some insights into the reaction mechanism, although detailed the mechanistic study has been hampered by the instability of the peroxo intermediates. All experiments were run under anaerobic atmosphere and in nonhalogenated aprotic solvents such as pentane and toluene because some oxidative reactions induced by metal–peroxo species were known to involve radical intermediate.^{1,7f,13b,14f,28,29}

Many Co(III)–peroxo⁵ species can be isolated even at room temperature. Some of those compounds are known to show the capability of oxidation of hydrocarbons; however, such oxidation reactions proceed only at slightly higher temperature (≈ 60 °C).¹² In contrast, our Co(II)–peroxo species **2** and **3** are reactive even at low temperature. This result implies that a lower oxidation state metal center is more effective for O–O bond activation due to high electron-donating ability of the metal center to the peroxide. The LUMO of peroxide anion is σ^* orbital, and therefore, the back-donation from the metal center to the antibonding σ^* orbital weakens the O–O bond.^{7a–e,10}

In the present oxygenation, only the proximal isopropyl groups are functionalized and the distal Prⁱ groups remain unaffected even in the presence of an excess amount of H₂O₂. This result implies that the oxygenations take place within the coordination sphere of the metal ion. Recently, three examples of similar intramolecular oxidative reactions at the methine group of isopropyl substituents via μ -peroxo species have been reported.^{13b,14f,29} Tolman et al. have revealed that decomposition of the dinuclear Cu(II)– μ - η^2 : η^2 -peroxo complex bearing the Prⁱ₃TACN ligand results in the H-atom abstraction from the Prⁱ-methine group to give the bis(μ -hydroxo) complex,²⁹ whereas the Cu(III)₂-bis(μ -oxo) complex, which is in equilibrium with the Cu(II)₂- μ - η^2 : η^2 -peroxo complex, induces the oxidative N-dealkylation.¹¹ Very recently, Sorrell et al. have reported that the Cu(II)₂- μ - η^2 : η^2 -peroxo complex with the tris(imidazolyl)phosphine ligand, whose structure may be very similar to that of our previous oxyhemocyanin model complex,³⁰ decomposes to induce the oxygenation of the Prⁱ group.^{14f} An example closely related to our results have been shown by Theopold and co-workers; the thermal decomposition of monomeric Co(II)–superoxo complex with the similar hydrotris(pyrazolyl)borate, HB(3-Prⁱ-5-Mepz)₃, results in H-atom abstraction from the proximal Prⁱ group associated with the O–O bond cleavage of the dinuclear Co(II)– μ -peroxo intermediate; however, no oxygenated products but the isopropenyl compound is yielded.^{13b} In both of the Tolman's and Theopold's systems, the H-atom abstraction process giving tertiary alkyl radical species is involved in the rate-determining step. In our system, a tertiary alkyl radical intermediate is also presumed to be formed.

The most important point of our result is that the present oxygenation reaction is dependent on the structure of the peroxo species;⁵ i.e., decomposition of the μ -peroxo complex **2** and the alkylperoxo complex **3** results in the mono-oxygenated **4**

and the dioxygenated **5**, respectively.³¹ On the basis of these observations, we propose plausible mechanisms involving the Co^{II}OOX (X = Co(II), alkyl) species as key intermediates. One possible “radical coupling” reaction pathway which is included in “radical-involving” mechanisms consists of following steps: (1) homolytic O–O bond rupture of the CoOOX species gives the Co–O• and X–O• intermediates, (2) abstraction of the methine hydrogen atom in the proximal Prⁱ group with X–O• generates the *tert*-alkyl radical center, and (3) coupling of the resulting *tert*-alkyl radical center with the Co–O• moiety furnishes the chelating alkoxide structure (Schemes 3 (path A) and 5). A “classical OH rebound” reaction pathway is also classified into the part of the “radical-involving” mechanisms (Scheme 3). In the decomposition process of **2**, not only the mono-oxygenated compound **4** but also **1**, in which the Prⁱ groups are unfunctionalized, is obtained; however, the dioxygenated bis(μ -alkoxo) complex **5** is not yielded. Therefore formation of the μ -alkoxo- μ -hydroxo core of **4** may proceed with retention of the bimetallic structure, and it also suggests the possibility of concerted H-atom abstraction with O–O bond rupture.³² The formation of the mono-oxygenated **4** and non-functionalized **1** indicates the existence of two or more different “radical-involving” reaction pathways; one possible explanation is existence of two different routes so-called “one methine attacked” route (path A–C) and “two methines attacked” route (path D) arising from the highly symmetric structure of **2**. Another possible pathway via the diradical intermediate (i.e., **2'** → C, D) involves classical “rebound” process of OH group (resulting from H atom abstraction by Co^{II}–O•) to the methine carbon radical followed by oxidation of a resulting Co(I) species. On the basis of the low yield of the oxygenation product **4**,³³ competition between the OH rebound and the H atom abstraction by the resulting alkyl radical is a possible event. The hydrogen atoms of hydroxide groups in **4** and **1** are concluded to come from the methine groups because no OD complexes are obtained upon decomposition of **2** in toluene-*d*₈, and the remaining *tert*-alkyl radicals probably abstract the hydrogen atoms from the solvent or H₂O.^{29,34} These results consistent with each pathways presented in Scheme 3.

Another possible mechanism involves the dinuclear Co(III)–bis(μ -oxo) intermediate **2''**, which is an alternative resonance structure of the dinuclear Co^{II}–O• intermediate **2'**, as the similar oxygenation mechanism proposed by Tolman et al.^{11d,f} (“oxo-transfer” mechanisms in Scheme 4). The proximal H atom is abstracted by the Co–oxo species, and “rebound” between the resulting tertiary alkyl radical and the OH radical followed by hydrolysis and dehydrative condensation furnishes the final

(31) In Sorrell's system, stoichiometric oxygenation is also observed, i.e., one molecule of the dinuclear Cu(II)– μ - η^2 : η^2 -peroxo complex results in the ligand-mono-oxygenated compound and the hydroxo complex. See ref 14f.

(32) On the basis of the short lifetime of an alkyl radical, concerted oxygenation mechanisms are proposed: (a) Elliott, S. J.; Zhu, M.; Tso, L.; Nguyen, H.-H. T.; Yip, J. H.-K.; Chan, S. I. *J. Am. Chem. Soc.* **1997**, *119*, 9949. (b) Choi, S.-Y.; Eaton, P. E.; Hollenberg, P. F.; Liu, K. E.; Lippard, S. J.; Newcomb, M.; Putt, D. A.; Upadhyaya, S. P.; Xiong, Y. *J. Am. Chem. Soc.* **1996**, *118*, 6547.

(33) Because of similar characteristics (paramagnetism, mass number) of the reaction products, we could not determine accurate products yields by analysis of the crude reaction mixture. Thus, the yields of products were determined by isolation of the products in the present study.

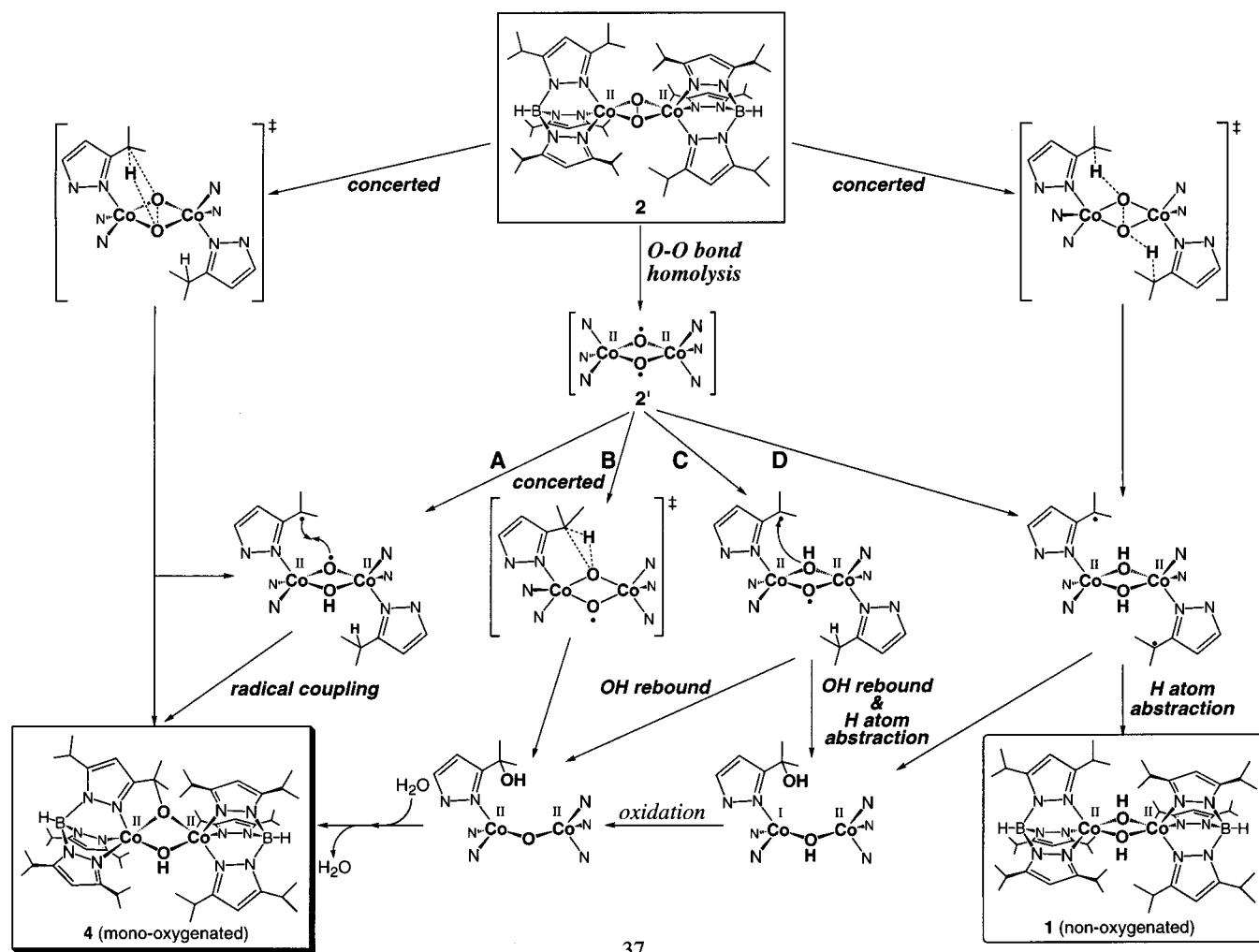
(34) FD-MS analysis of the products obtained by decomposition of **2** in toluene-*d*₈ revealed that the increase of ion peaks at 1111 and 1110, which were attributed to two and/or one deuterium-incorporated μ -carbonato complex formed by reaction of atmospheric CO₂ with the corresponding non-oxygenated bis(μ -hydroxo) complexes **1**. However, further analysis of resulting pyrazoles (which would be obtained by degradation of the product complexes) and determination of deuterium incorporation yields were not performed.

(28) Kitajima, N.; Koda, T.; Iwata, Y.; Moro-oka, Y. *J. Am. Chem. Soc.* **1990**, *112*, 8833.

(29) Mahapatra, S.; Halfen, J. A.; Wilkinson, E. C.; Que, L., Jr.; Tolman, W. B. *J. Am. Chem. Soc.* **1994**, *116*, 9785.

(30) Sorrell, T. N.; Allen, W. E.; White, P. S. *Inorg. Chem.* **1995**, *34*, 952.

Scheme 3



product **4**. In the case of this mechanism, concerted oxygen atom transfer via a transition state in which the oxo group interacts with both the carbon and hydrogen atoms of the Pr^i -methine group should be also taken into consideration.^{11d,f,32}

In contrast, the alkylperoxo complex **3** is monomeric; thus, the decomposition of **3** may proceed via a monomeric intermediate and final dimerization leads to the stable five-coordinated structure of the bis(μ -alkoxo) complex **5** (Scheme 5). As found in the decomposition of **2**, the nonfunctionalized bis(μ -hydroxo) complex **1** is also yielded, but the mono-oxygenated complex **4** is never obtained from the alkylperoxo complex **3**. These results imply that scrambling of the hydroxo complex **1** with the monomeric alkoxo intermediate **5'** was excluded.

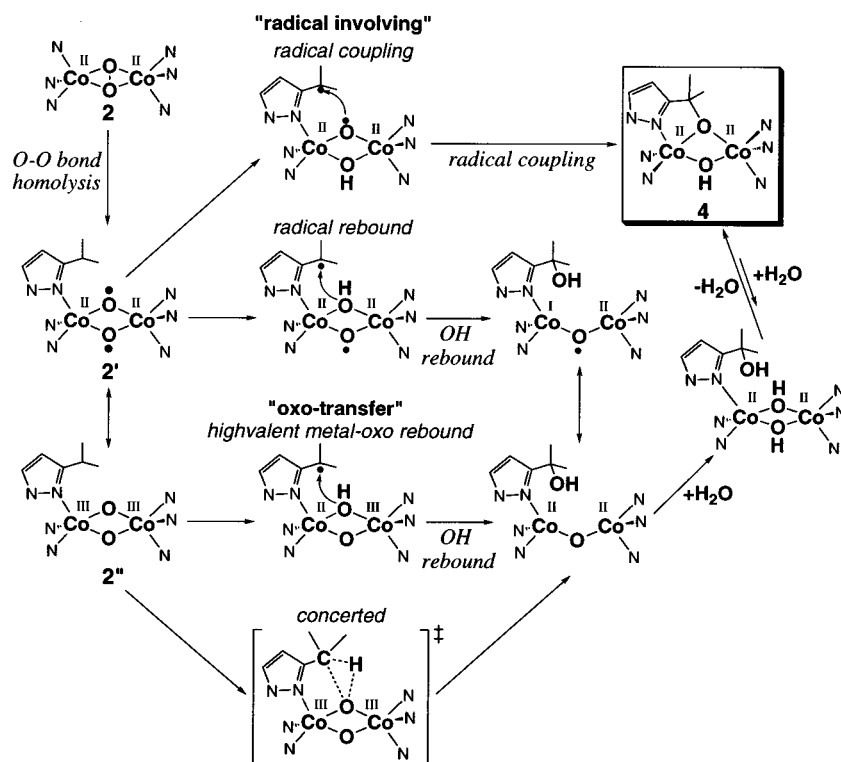
The decomposition of the μ -peroxo complex **2** in the presence of excess H_2O_2 yielded the dioxygenated bis(μ -alkoxo) complex **5**³⁵ and the fully oxygenated hydroxo-alcohol complex **6**, but no mono-oxygenated μ -alkoxo- μ -hydroxo complex **4**. Therefore, the present oxygenation giving the fully oxygenated complex **6** may proceed via $\text{Co}^{\text{II}}\text{-OOH}$ intermediates in a stepwise manner. It is notable that **6** is obtained by the reaction of the isolated **5** with H_2O_2 , but the reaction of **1** or **5** with alkyl hydroperoxides under various conditions failed in full oxygenation. These observations imply that the formation of **6** may be achieved by repetitious oxygenation via monomeric hydroperoxo intermediates as presented in Scheme 6. H_2O_2 , which is more acidic than ROOH ($\text{R} = \text{Bu}^i, \text{PhMe}_2\text{C}$), replaces the alkoxide ligand in the monomeric alkoxo compound **5'** to

form the hydroperoxo intermediate, by which another proximal Pr^i group is oxygenated to give a monomeric dioxygenated product. Repetition of the oxygenation process would furnish **6** after coordination of one of the resulting alcohol groups and the hydroxide. Examination of catalytic activity of the present system is now under way.

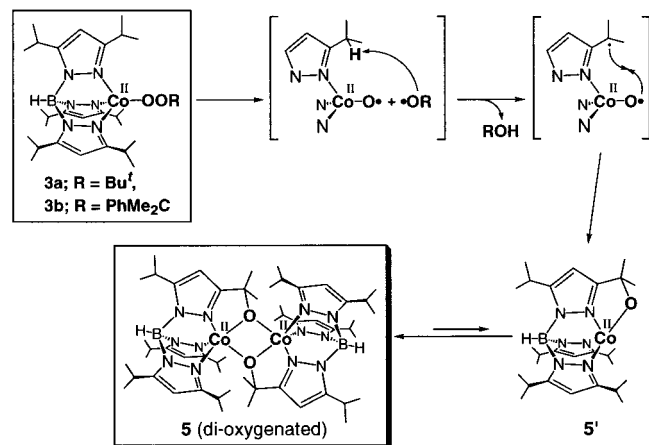
Finally, our result suggests a simple, but important point for the design of catalysts: substrates must be placed at an appropriate position where reactive oxygen species can be

(35) In the case of the decomposition of **2** in the presence of excess H_2O_2 , two possible reaction pathways can be drawn. One pathway may proceed via a monomeric $\text{Co}(\text{II})$ -hydroperoxo intermediate which must be similar to the alkylperoxo complex **3**; protonolysis of the $\text{Co}-\text{O}$ part of **2** with H_2O_2 forms 2 equiv of the mononuclear hydroperoxo species. Subsequent radical processes analogous to those mentioned in Scheme 5 give the chelating alkoxo intermediate **5'**, dimerization of which gives the dioxygenated product **5**. Another pathway involves the mono-oxygenated complex **4** as a precursor; dehydrative condensation of the OH ligand of **4** and H_2O_2 results in a (μ -alkoxo)(μ -hydroperoxo) intermediate, or replacement of the μ -alkoxide moiety by H_2O_2 followed by reaction with the OH moiety yields a reactive dinuclear $\text{Co}(\text{II})$ μ -peroxo species (similar to **2**) having a monohydroxylated tris(pyrazolyl)borate ligand. Both intermediates can oxidize a Pr^i group by similar manners shown in Scheme 3 or 4 (μ -peroxo intermediate) or Scheme 5 (μ -hydroperoxo intermediate). We examined reaction of the isolated **4** with H_2O_2 under various conditions. At low temperature (-50°C), **4** did not react with H_2O_2 (no spectral change was observed) and no further ligand oxygenated compounds were obtained, although room-temperature reaction yielded **5** (and **6**). However, detections of any peroxo species failed because the reactions occurred only at the room temperature. In conclusion, we cannot determine the decomposition pathway of **2** in the presence of excess H_2O_2 yielding **5**, although the possibility of the stepwise oxygenation route (i.e., **4** (mono-oxygenated) \rightarrow **5** (dioxygenated)) cannot be ruled out.

Scheme 4



Scheme 5

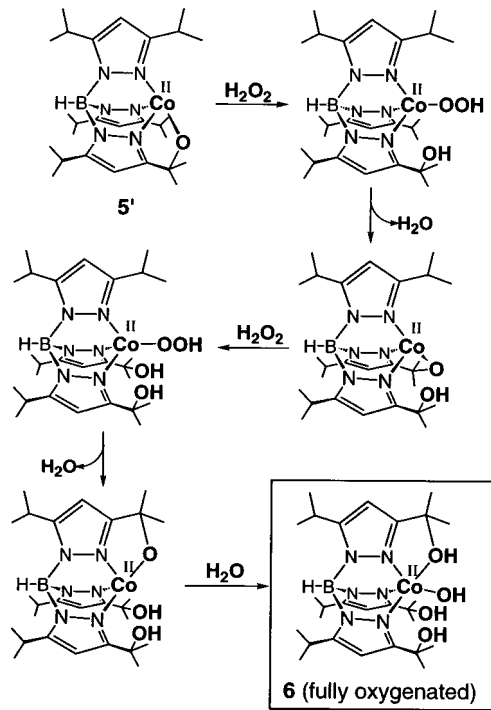


accessible. On the basis of these findings, we are planning a study on new Co(II) catalyst which is able to oxidize alkane. In addition, investigations of the reaction mechanism (kinetic study) and the more detailed characteristics of Co(II) peroxo species are under study by using similar ligand systems.

Concluding Remarks

In the present study, we have succeeded in isolation and structure determination of the aliphatic C–H bond oxygenated compounds resulting from decomposition of the Co(II)–peroxo species.⁵ Only the proximal Prⁱ groups are oxygenated even in the presence of an excess amount of ROOH, suggesting that the present oxygenations proceed within the metal-coordination sphere. The number of oxygen atoms incorporated into the tris-(pyrazolyl)borate ligand depends on the kind of the peroxo species (i.e., μ -peroxo or alkylperoxo) and the reaction conditions (i.e., the amount of H₂O₂). We propose the plausible ligand oxygenation mechanisms, so-called “radical involving”, “oxo-transfer”, and “concerted” mechanisms. In the “radical-

Scheme 6



involving” mechanism, the two oxyl radical species resulting from homolytic O–O bond rupture abstract a hydrogen atom from the isopropyl group to provide the alcohol functional groups by coupling with the resulting tertiary alkyl radical. In the mono-oxygenation reaction (i.e., **2** → **4**), the “oxo-transfer” mechanism, which involves H-atom abstraction and rebound of a resulting OH by dinuclear Co(III)–bis(μ -oxo) intermediate, is also possible. In the “concerted” mechanism, the oxygenation proceeds via a transition state in which the O–O and C–H bonds are activated simultaneously (analogue of “radical involv-

ing” mechanism) or the oxo group interacts with both the carbon and hydrogen atoms of the Prⁱ-methine group (analogue of “oxo-transfer” mechanism). The structure of the alkylperoxo complex of Co(II) was successfully revealed for the first time by using the highly hindered HB(3-Bu^t-5-Prⁱpz)₃ ligand.

Acknowledgment. This research was supported in part by a Grant-in-Aid for Specially Promoted Scientific Research (No.

08102006) from the Ministry of Education, Science, Sports and Culture of the Japanese government.

Supporting Information Available: Summary of X-ray analysis, atomic coordinates, thermal parameters, and bond lengths and angles for **4**, **5**, **6**, and **9**. NMR spectra of **4**, **5**, and **6** (39 pages, print/PDF). See any current masthead page for ordering information and Web access instructions.

JA9720523